Geography Compass 2/6 (2008): 1943–1961, 10.1111/j.1749-8198.2008.00182.x

Hyperspectral Remote Sensing of Vegetation

Jungho Im[1]* and John R. Jensen[2]
[1]*State University of New York, College of Environmental Science and Forestry*
[2]*University of South Carolina*

Abstract

Hyperspectral analysis of vegetation involves obtaining spectral reflectance measurements in hundreds of bands in the electromagnetic spectrum. These measurements may be obtained using hand-held spectroradiometers or hyperspectral remote sensing instruments placed onboard aircraft or satellites. Hyperspectral remote sensing provides valuable information about vegetation type, leaf area index, biomass, chlorophyll, and leaf nutrient concentration which are used to understand ecosystem functions, vegetation growth, and nutrient cycling. This article first reviews hyperspectral remote sensing and then describes current modeling and classification techniques used to estimate and predict vegetation type and biophysical characteristics.

Introduction

Vegetation covers much of the terrestrial surface and consists mainly of five landscapes, including: agriculture, forest, rangeland, wetland, and urban vegetation (Jensen 2007). Monitoring vegetation through time is very important for many earth resource management applications. Monitoring is often conducted by taking detailed *in situ* biophysical and biochemical measurements through time at the leaf (foliar) or canopy level (e.g. Chmura et al. 2007; Mutanga et al. 2003; Tilling et al. 2007). Unfortunately, traditional *in situ* vegetation measurement is labor-intensive, time-consuming, and often difficult to conduct or extrapolate over large geographic areas.

Conversely, *remote sensing*, the collection of information about an object without being in direct physical contact with the object, is now a viable alternative for monitoring numerous vegetation characteristics. Scientists have worked for the past 40 years documenting robust relationships between *in situ* vegetation measurements and remote sensing-derived measurements to predict or monitor vegetation biophysical and biochemical characteristics (e.g. Beeri et al. 2007; Chirici et al. 2007; Gong et al. 2002; Hu et al. 2004; Johnson et al. 1994; Perry and Davenport 2007; Wu et al. 2008). Two significant advances have helped to make this capability possible:

(i) improvement in hand-held spectroradiometers, and (ii) the development of hyperspectral remote sensing systems that can be used to perform imaging spectrometry.

In situ spectroradiometers can be used to provide a high-resolution reflectance spectrum for a material under investigation (e.g. vegetation, soil, water, rock) every 1–3 nm in the region from 400 to approximately 2500 nm. *In situ* spectral reflectance measurement in the field takes place at very specific locations (i.e. point measurements). It is difficult to extrapolate these point measurements through space (or time).

Remote sensing instruments have matured from simple panchromatic (single-band) measurements to more sophisticated multispectral measurements (e.g. 2 to 15 bands), to present day hyperspectral remote sensing in literally hundreds of bands in the electromagnetic spectrum. Imaging spectroradiometers placed onboard suborbital aircraft (e.g. NASA's Airborne Visible/Infrared Imaging Spectrometer [AVIRIS]) or satellites (e.g. NASA's Hyperion sensor) provide an image data cube with a reflectance spectrum for each picture element within the image. Imaging spectroradiometers usually have relatively lower spectral resolution (e.g. 10 nm) than hand-held spectroradiometers, but it is generally sufficient to identify the characteristics of surface materials, such as soils, rocks, water, and vegetation, because many of the materials under investigation have unique absorption features that are often only 10–20 nm wide (Curran et al. 1995; Jensen 2007). Hyperspectral measurements obtained using airborne imaging spectrometry now provide valuable information regarding the dynamics of foliar and/or canopy characteristics that is necessary to understand how ecosystems function, vegetation grows, and nutrients are cycled. Many studies have focused on remote sensing of leaf area index (LAI), biomass, chlorophyll, and leaf nitrogen concentration (e.g. Townsend et al. 2003; Wu et al. 2008). Less research has been performed to measure leaf nutrients and trace elements, such as phosphorus, potassium, calcium, and magnesium (e.g. Ferwerda and Skidmore 2007; Mutanga et al. 2003). Hyperspectral remote sensing has been also used to map vegetation species and to measure the proportion (abundance) of materials within pixels (e.g. Kokaly et al. 2003; Jia et al. 2006; Okin et al. 2001).

This article consists of four sections that review: (i) the fundamentals of hyperspectral remote sensing; (ii) key vegetation characteristics highly related to vegetation quality and functional health, (iii) modeling techniques used to estimate and predict the key vegetation biophysical and biochemical characteristics, and (iv) methods of hyperspectral vegetation mapping and subpixel processing.

In Situ *(Hand-Held) and Remote Sensing Spectroradiometry*

Both *in situ* hand-held spectroradiometers and hyperspectral remote sensing instruments have a common characteristic. They collect reflected or emitted

Fig. 1. Scientists taking *in situ* spectral reflectance measurements of a *Spectralon* plate (reference) prior to collecting *in situ* spectral reflectance measurements of a nearby vegetation (target).

data in many relatively narrow, contiguous, and/or noncontiguous spectral wavelengths throughout the ultraviolet, visible, and/or infrared regions of the electromagnetic spectrum (Jensen 2005, 2007).

IN SITU (HAND-HELD) SPECTRORADIOMETRY

Scientists use hand-held spectroradiometers to collect reflected or emitted radiant flux from selected materials (e.g. vegetation) about 1 m above the materials. The measurements may be made in the field (Figure 1) or in the laboratory. For example, the spectral reflectance characteristics of *Bahiagrass* recorded using a hand-held spectroradiometer in the region from 350 to 1050 nm are shown in Figure 2. Some scientists suggest that such spectral information constitutes a spectral signature of the material (i.e. a spectral fingerprint of the material). Other scientists say that this should not be considered a definitive spectral signature (fingerprint), because there is so much variability in nature. For example, the spectral reflectance characteristics of a *Sycamore* leaf obtained in the field in May in Virginia will likely be

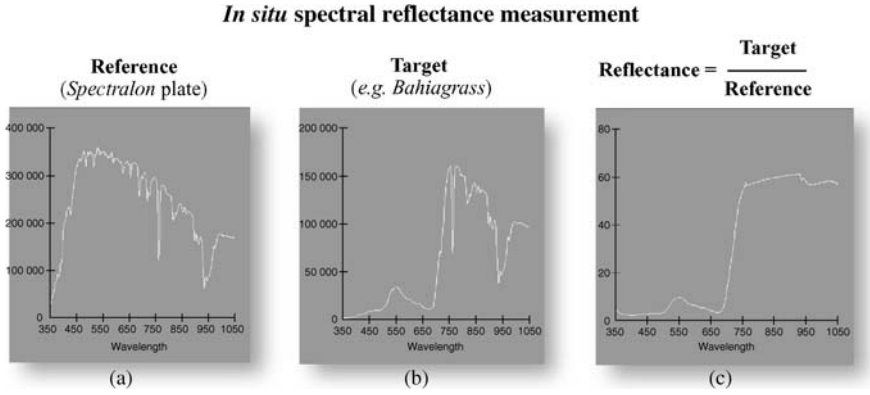

Fig. 2. A spectral reflectance curve of *Bahiagrass* obtained by dividing *Bahiagrass* target spectra by the *Spectralon* plate reference spectra (modified from Jensen 2007).

somewhat different from the spectral reflectance of exactly the same leaf measured in the same field in July. Similarly, the spectral reflectance characteristics of a typical *Sycamore* leaf measured in May in Virginia might not look exactly like the spectral reflectance of a typical *Sycamore* leaf measured in May in South Carolina. The phenological stage of development, percent soil moisture, percent plant moisture, percent canopy closure, and man-made influences (e.g. row spacing and orientation) are just a few of the factors that can cause the same vegetation type (e.g. corn) to have somewhat different spectral reflectance characteristics even within the same geographic area.

The spectral reflectance data acquired using *in situ* hand-held spectroradiometers are generally used to (i) document the spectral reflectance characteristics of materials such as vegetation, (ii) calibrate multispectral/hyperspectral remote sensing data to minimize atmospheric scattering and absorption, and (iii) perform matched-filtering whereby *in situ* reflectance characteristics of known materials are used to identify the same materials in hyperspectral remote sensor data (Goetz 2002; Jensen 2007).

IMAGING SPECTRORADIOMETERS USED FOR HYPERSPECTRAL REMOTE SENSING

Hyperspectral remote sensing involves placing a spectroradiometer onboard an aircraft or spacecraft and pointing its optics toward the ground. Two approaches to hyperspectral remote sensing include the use of (Figure 3): (i) whiskbroom and (ii) linear and area array technology (Jensen 2007). Linear and area array sensors generally have improved image geometry, because there is no rapidly moving scanning mirror present to introduce geometric distortion. They also have improved radiometry because each detector can record reflected or emitted energy for a longer period of time for the geographic area of interest (i.e. the area within the instantaneous

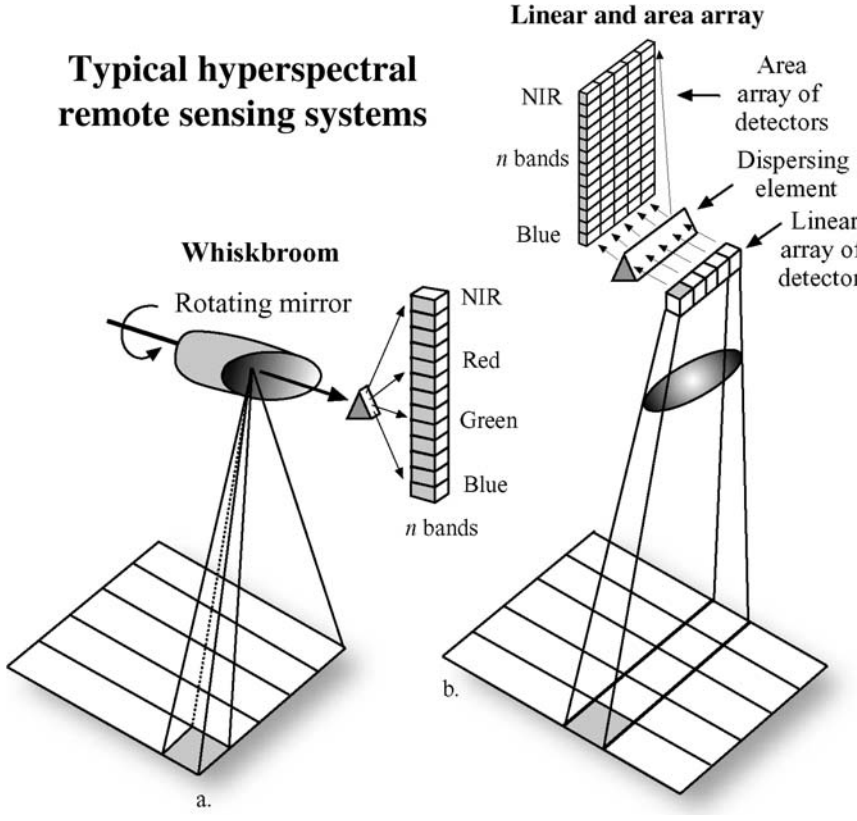

Fig. 3. Typical hyperspectral remote sensing systems based on (i) whiskbroom, and (ii) linear and area array technology (modified from Jensen 2005).

field of view of the sensor system). Hyperspectral imagery of forest plots on the Savannah River Site near Aiken, South Carolina, is shown in Figure 4.

Hyperspectral remote sensing data provide much more detailed spectral information of an area when compared with typical multispectral sensors which collect information in just a few broad spectral bands (e.g. Landsat Enhanced Thematic Mapper). Such detailed spectral information can be used to identify specific materials within a pixel based on the reflectance characteristics (e.g. Haboudane et al. 2002; Nolin and Dozier 2000). Both *in situ* spectroradiometer and hyperspectral remote sensing measurements have been widely used together in diverse applications, such as in forestry, geology, hydrology, atmospheric science, and geography.

Vegetation Biophysical and Biochemical Characteristics

Several vegetation biophysical and biochemical characteristics that can be remotely sensed are listed in Table 1.

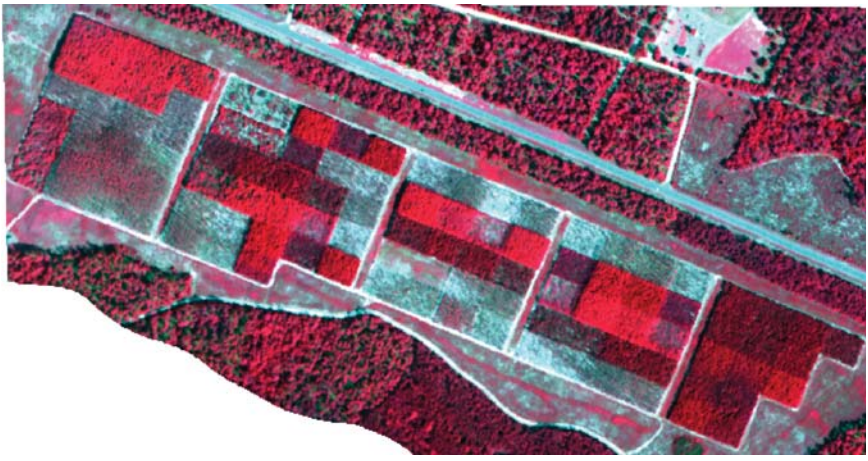

Fig. 4. Color composite of three bands of hyperspectral imagery (RGB = bands 40, 30, 20) of forest plots on the Savannah River Site near Aiken, South Carolina. The 1×1 m spatial resolution 63-band imagery was acquired by an Airborne Imaging Spectrometer for Applications (AISA+) Eagle sensor system in the wavelength interval 400 to 980 nm on September 15, 2006.

Table 1. Major biophysical and biochemical characteristics of vegetation.

- Leaf area index
- Chlorophyll *a* and *b*
- Canopy structure and height
- Absorbed photosynthetically active radiation (*APAR*)
- Biomass
- Water content
- Leaf nutrients concentrations (e.g. N, P, K, Ca, Mg)
- Evapotranspiration

LEAF AREA INDEX

Leaf area index (LAI) is defined as the total area of one-sided green leaves in relationship to the ground below them (FAO 2005; Jensen 2007). Because LAI directly quantifies the vegetation canopy structure, it is highly related to diverse canopy processes, including water interception, photosynthesis, evapotranspiration, and respiration. Thus, LAI information can be used in various terrestrial monitoring and modeling applications to help quantify the processes.

CHLOROPHYLL CONCENTRATION

The chlorophyll concentration in vegetation is mainly responsible for the absorption of photosynthetically active radiation (PAR). A high degree of

inter-correlation between canopy photosynthetic rates, LAI, absorbed PAR, and chlorophyll concentrations is normal in natural ecosystems (Boegh et al. 2002; Jensen et al. 1998, 2002). The two optimum spectral regions for sensing the chlorophyll absorption characteristics of a leaf are believed to be in the blue (450 to 520 nm) and red (630 to 690 nm) portions of the spectrum. The former region is characterized by strong absorption by carotenoids and chlorophylls, whereas the latter is characterized by strong chlorophyll absorption (Jensen 2005; Sims and Gamon 2002).

BIOMASS

The amount of dead and live biomass is directly related to the productivity of vegetation (e.g. in agricultural crops). *In situ* biomass measurement generally involves measuring the biomass for various parts of the plant (e.g. root, stem, leaf).

WATER CONTENT

Because water present in the spongy mesophyll of a plant absorbs much of the energy in the mid-infrared spectral region, remote sensing techniques have been used to identify leaf water content. Hence, as the water content of vegetation increases, the reflectance generally decreases in the mid-infrared regions. For example, Figure 5 illustrates how the spectral reflectance of *Bahiagrass* changes according to various irrigation treatments (Garcia-Quijano 2006).

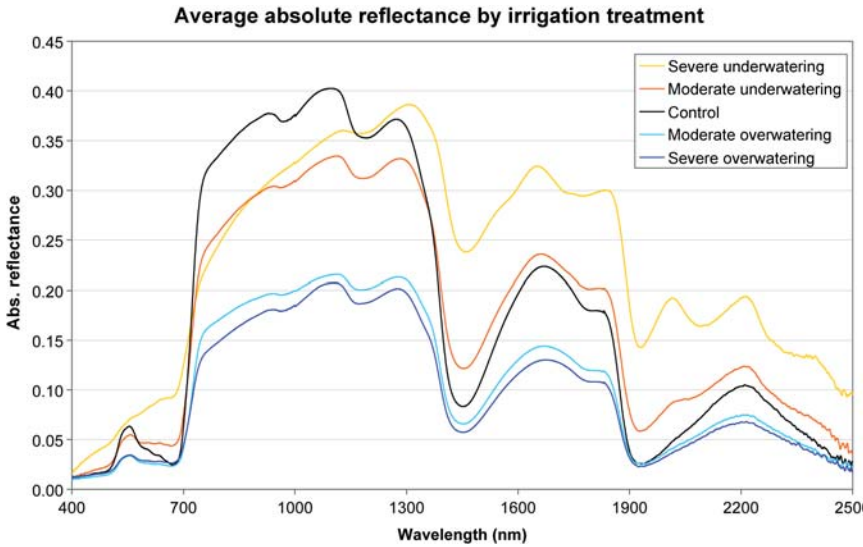

Fig. 5. Spectral reflectance curves of *Bahiagrass* subjected to various irrigation treatments measured using an *in situ* ASD FieldSpec3 JR spectroradiometer (Garcia-Quijano 2006).

SOIL NUTRIENT AVAILABILITY

The productivity and quality of vegetation are affected by soil nutrient availability, which in turn influences leaf nutrient concentration (Townsend et al. 2003). Leaf nutrients include nitrogen, phosphorus, potassium, calcium, and magnesium. Nitrogen has been explored by many scientists using hyperspectral remote sensing techniques because it is a major nutrient of vegetation. Other nutrients, however, have had relatively less exploration because leaf nutrient levels vary by differences in the physical structure of canopies and there may be no strong linear relationship between spectral signature-derived values and the nutrient levels. Phosphorus and potassium, critical to vegetation growth, are used in various mechanisms, such as fat formation, energy transfer, cell division, and seed sprouting (Jokela et al. 1997; Milton et al. 1991).

Methods Used to Model Vegetation Foliar/Canopy Characteristics

Several approaches have been investigated to estimate the biophysical and biochemical characteristics of vegetation using hand-held spectroradiometer measurements and/or hyperspectral remote sensing measurements. These approaches include: (i) statistical regression methods, (ii) spectral positioning methods, (iii) physical modeling, and (iv) artificial intelligence.

STATISTICAL REGRESSION APPROACH

Numerous scientists have used regression analysis to correlate *in situ* biophysical/biochemical measurements with remote sensing-derived reflectance values or vegetation indices (e.g. Johnson et al. 1994; Tilling et al. 2007; Ye et al. 2006). Statistical regression techniques used include simple linear regression, multiple regression, principal component regression, and partial least squares regression. Principal component regression combines principal component analysis and inverse least squares regression to generate a predictive model for given samples. It first converts a number of independent variables to principal components through an orthogonal linear transformation. Typically, a meaningful subset of the principal components is used to estimate the regression coefficients.

Partial least squares regression combines principal component analysis and multiple regression. Like principal component regression, partial least squares regression reduces the dimensionality of independent variables to a few manageable non-correlated variables using component projection. These non-correlated variables represent the relevant latent structural information of the independent variables for predicting the dependent variable, such as vegetation chlorophyll concentration (Hansen and Schjoerring 2003).

Some studies have used the spectral reflectance data for the regression analyses, while others have summarized the remote sensing-derived

information into vegetation indices and then adopted statistical regression approaches. Some scientists have reported that specialized hyperspectral vegetation indices are useful for estimating vegetation characteristics, such as LAI, biomass, chlorophyll, and nitrogen concentration (e.g. Aparicio et al. 2000; Hansen and Schjoerring 2003). There are many types of vegetation indices applicable for hyperspectral analysis (Jensen 2007). Some vegetation indices widely used for modeling the characteristics and functional health of vegetation are listed in Table 2.

Gong et al. (2002) reported correlation analysis results between *in situ* hand-held spectroradiometer measurements and three foliage nutrient constituents (i.e., nitrogen, phosphorus, and potassium). The hyperspectral data were evaluated using univariate correlation and multivariate regression methods with several different explanatory variables, such as vegetation indices, principal component-based values, and first-order derivative spectra. Hyperion and AVIRIS imagery were used to model nitrogen concentration for mixed oak forests in Maryland at the canopy level (Townsend et al. 2003). They utilized partial least squares regression of first derivative reflectance to produce robust and very similar prediction results between the two image datasets. The study suggested that nitrogen might be estimated using satellite hyperspectral remote sensing data as well as airborne data. Ferwerda and Skidmore (2007) used field spectrometry to estimate the nutrient status (i.e. nitrogen, phosphorus, calcium, potassium, sodium, and magnesium) of four woody plant species. They utilized a stepwise regression technique to predict the six nutrients with three different explanatory variables (i.e. reflectance, derivative, and continuum-removed spectra).

SPECTRAL POSITIONING

Wavelength position, not the spectral reflectance itself, is a major concern when using the spectral positioning approach to hyperspectral data analysis (Gong et al. 2002). For example, the *red-edge position*, a unique characteristic of typical vegetation spectral response, is defined as the spectral position between the red (~680 nm) and near-infrared (~800 nm) wavelengths where the maximum slope is found (Gong et al. 2002; Jensen 2007). It is very sensitive to the biophysical and biochemical properties of vegetation, such as LAI, chlorophyll content, and biomass (Cho and Skidmore 2006; Curran et al. 1995). A shift in the red-edge position may be due to phenological change and/or vegetation stress.

Unlike the vegetation indices based on band ratios or band combinations, many contiguous bands may be used to derive the red-edge when analyzing hyperspectral data. There are several methods for red-edge positioning. Many studies locate the red-edge wavelength using derivative functions by extracting the highest peak from the first derivative of the hyperspectral reflectance data (e.g. Filella and Penuelas 1994; Horler et al. 1983). Other scientists use a Gaussian model to identify the red-edge position (e.g.

Table 2. Various vegetation indices used to model vegetation quality and functional health using hyperspectral data (adapted from Jensen 2007).

Vegetation index	Equation	Description	Reference
Near-infrared/red ratio	$Ratio = \frac{\rho_{nir}}{\rho_{red}} = \frac{\rho_{900nm}}{\rho_{660nm}}$	Ratio is highly correlated with vegetation LAI and biomass.	Colombo et al. (2003)
Normalized difference vegetation index (NDVI)	$NDVI = \frac{\rho_{nir} - \rho_{red}}{\rho_{nir} + \rho_{red}} = \frac{\rho_{900nm} - \rho_{660nm}}{\rho_{900nm} + \rho_{660nm}}$	Scientists using hyperspectral data may select among numerous red and NIR hyperspectral bands to use in the NDVI algorithm.	Huete et al. (2002)
MODIS enhanced vegetation index (EVI)	$EVI = G\frac{\rho_{nir} - \rho_{red}}{\rho_{nir} + C_1\rho_{red} - C_2\rho_{blue} + L}(1+L)$ where the coefficients G, C_1, C_2, and L are empirically determined as 2.5, 6.0, 7.5, and 1.0 respectively.	Developed for use with MODIS data. It includes a soil background reflectance factor and corrects for atmospheric aerosol scattering (Jensen 2007).	Huete et al. (2002)
Soil and atmospherically resistant vegetation index (SARVI)	$SARVI = \frac{\rho_{nir} - \rho_{rb}}{\rho_{nir} + \rho_{rb} + L}$ where, $\rho_{rb} = \rho_{red} - \gamma(\rho_{blue} - \rho_{red})$ and γ is normally equal to 1.0 in order to minimize atmospheric effects.	Developed by adding the L function and normalizing the blue band in ARVI. It is less sensitive to noise by soil and atmospheric effects.	Huete and Liu (1994)
Visible atmospherically resistant index (VARI)	$VARI_{green} = \frac{\rho_{green} - \rho_{red}}{\rho_{green} + \rho_{red} - \rho_{blue}} = \frac{\rho_{560nm} - \rho_{660nm}}{\rho_{560nm} + \rho_{660nm} - \rho_{460nm}}$	Less sensitive to atmospheric effects. It is useful when extracting vegetation fraction information over large areas.	Gitelson et al. (2002)
Normalized difference moisture or water index (NDWI)	$NDWI = \frac{\rho_{nir} - \rho_{midIR}}{\rho_{nir} + \rho_{midIR}} = \frac{\rho_{860nm} - \rho_{1240nm}}{\rho_{860nm} + \rho_{1240nm}}$	Useful when extracting vegetation water content information. It was originally based on Landsat TM NIR and middle-infrared bands.	Galvao et al. (2005)
Transformed chlorophyll absorption ratio index/ optimized soil-adjusted vegetation index (TCARI/ OSAVI)	$TCARI = 3\left[\rho_{700} - \rho_{670} - 0.2(\rho_{700} - \rho_{550})\left(\frac{\rho_{700}}{\rho_{670}}\right)\right]$ $OSAVI = \frac{(1+0.16)(\rho_{800} - \rho_{670})}{(\rho_{800} + \rho_{670} + 0.16)}$	Minimizes soil background effects and is sensitive to chlorophyll concentration.	Haboudane et al. (2002)

Geography Compass 2/6 (2008): 1943–1961, 10.1111/j.1749-8198.2008.00182.x

Miller et al. 1990; Pinar and Curran 1996). Some studies have found that the red-edge position is not a single location, but multiple wavelengths (e.g. Horler et al. 1983; Smith et al. 2004). Two representative red-edge positioning techniques are:

- *Linear Red-Edge Position (REP)* (Dawson and Curran 1998):

$$Linear\ REP = 700 + 40\left[\frac{\rho_{red-edge} - \rho_{700nm}}{\rho_{740nm} - \rho_{700nm}}\right], \text{ where } \rho_{red-edge} = \frac{\rho_{670nm} + \rho_{780nm}}{2}$$

- *Red-Edge Position Based on Derivative Ratio* (Smith et al. 2004):

$$\rho_{red-edge(725/702nm)} = \frac{(\rho_{726_{smooth}} - \rho_{724_{smooth}})/2}{\rho_{703_{smooth}} - \rho_{701_{smooth}})/2}, \text{ where}$$

$$\rho_{\lambda_{i,smooth}} = \frac{0.25 \cdot \rho_{\lambda_{i-2}} + 0.5 \cdot \rho_{\lambda_{i-1}} + \rho_{\lambda_i} + 0.5 \cdot \rho_{\lambda_{i+1}} + 0.25 \cdot \rho_{\lambda_{i+2}}}{0.25 + 0.5 + 1 + 0.5 + 0.25}.$$

In the red-edge positioning approach by Smith et al. (2004), individual reflectance data are first smoothed using a weighted mean moving average function. The function used a 5-nm sample range, which consisted of five values along the reflectance continuum. The relative weights of 0.25, 0.5, 1, 0.5, and 0.25 were applied to the values of the reflectance continuum to compute the average value. The derivative was then calculated by dividing the difference between two averaged reflectance values with a 2-nm interval. Additional methods used to determine the red-edge position are summarized in Baranoski and Rokne (2005).

PHYSICAL MODELING

Physical models are theoretically based on leaf scattering and absorption mechanisms associated with biochemistry (Gong et al. 2002). A representative type of model is the radiative transfer model, which simulates radiation transfer processes in vegetation by computing the interaction between plants and solar radiation. Biophysical and biochemical characteristics of vegetation can be retrieved through inversion of the radiative transfer model. Diverse inversion models have been investigated. Dawson et al. (1998) developed the Leaf Incorporating Biochemistry Exhibiting Reflectance and Transmittance Yields (LIBERTY) to model leaf biochemical characteristics, such as nitrogen, lignin, and cellulose, using reflectance spectra. Moorthy et al. (2008) used Compact Airborne Spectrographic Imager hyperspectral measurements to investigate the chlorophyll concentration of coniferous forests at the needle and canopy levels. They examined the pigment concentration at the needle level through the inversion of radiative transfer models, such as LIBERTY and PROSPECT, which are general radiative transfer plate models for leaf optical properties (Jacquemoud and Baret 1990). A turbid medium canopy model, SAILH, was used to estimate the

chlorophyll concentration at the canopy level. SAILH combined the SAIL reflectance model and the hotspot effect at the canopy level (Cheng et al. 2006). Darvishzadeh et al. (2008) used the PROSAIL canopy radiative transfer model (Jacquemoud and Baret 1990; Verhoef 1984) to predict the LAI and chlorophyll concentration in Mediterranean grassland. PROSAIL combines PROSPECT and the SAIL canopy bidirectional reflectance model.

Wavelet analysis can be used with radiative transfer models to better quantify biochemical characteristics of vegetation. For example, Blackburn and Ferwerda (2008) identified appropriate wavelet functions and coefficients in combination with two leaf radiative transfer models (i.e. LIBERTY and PROSPECT).

Vegetation water content can also be estimated using radiative transfer models. Colombo et al. (2008) utilized airborne Multispectral Infrared and Visible Imaging Spectrometer data to estimate the water content of poplar plantations based on empirical and radiative transfer models.

ARTIFICIAL INTELLIGENCE

Artificial intelligence has been used in hyperspectral remote sensing of vegetation based on neural networks and machine learning regression trees. Neural networks simulate the thinking process of the brain, which consists of numerous interconnected neurons used to process incoming information (Jensen et al. 1999; Hengl 2002). Neural networks have proven their potential especially when dealing with non-linear problems (e.g. Trombetti et al. 2008; Walthall et al. 2004; Ye et al. 2006). The biophysical and biochemical characteristics in a complex and dynamic environment may contain non-linear properties, wherein neural networks typically outperform conventional techniques.

Numerous types of neural networks have been applied to hyperspectral remote sensing data. Typical multilayer feed-forward backpropagation neural networks have been widely used for remote sensing applications. Sometimes, the determination of the topological structure of a neural network is a difficult task, often established by trial-and-error. Selection of the learning algorithm is also important. Basically, a learning algorithm finds optimum weights and biases by repeatedly updating existing ones with given parameters (Jensen et al. 1999).

A typical knowledge-based machine learning approach to modeling of continuous variables is regression trees, which use a binary recursive partitioning process (Breiman et al. 1984). Training samples (e.g. hyperspectral measurements from a known forest plot) are input to the regression trees to generate rule-based models for predicting a target variable through the recursive partitioning process. A split occurs if the model's combined residual error for two subsets is significantly lower than the residual error of the single best model in the process (Huang and Townshend 2003).

Advantages of machine learning regression trees include the ability to handle non-linear relationships between independent and dependent variables, and the use of both continuous and discrete variables as input data. A representative tool for machine learning regression trees is Cubist by *RuleQuest Inc.*, which uses a modified regression tree system to create rule-based predictive models from the data. Each rule has an associated multivariate linear model. These linear models are not mutually exclusive, allowing overlap between models. Output values are averaged to arrive at a final prediction. The predictability of Cubist has been examined in several studies (e.g. Huang and Townshend 2003; Moisen et al. 2006).

Many of the studies on hyperspectral modeling of vegetation characteristics have integrated neural network approaches and radiative transfer models. Trombetti et al. (2008) combined radiative transfer models and neural networks to retrieve vegetation canopy water content from MODIS data for the continental United States. They validated the models using AVIRIS data and determined that the neural network provided an improved basis for vegetation canopy water content over wide areas. Verger et al. (2008) combined radiative transfer models and the neural networks based on the Levenberg-Marquardt algorithm to estimate LAI. They concluded that the versatility and performance of neural networks for operational algorithms was promising. Several approaches to retrieve LAI from Landsat ETM+ data were evaluated by Walthall et al. (2004). The approaches included the combination of a radiative transfer model and neural network, scaled spectral vegetation indices (SVI) method, and empirical regression approaches using normalized difference vegetation index (NDVI) and SVI.

Im et al. (2008) investigated machine learning regression trees to model biophysical and biochemical characteristics of forest crops. They examined three approaches, including NDVI-based regression, partial least squares regression, and machine learning regression trees, to model several characteristics of forest crops with different nutrient and irrigation treatments. Good performance was achieved using partial least squares regression and machine learning regression trees in an environmentally complex forest site.

Vegetation Mapping and Spatial Pattern Analysis Using Hyperspectral Data

Previous sections described methods used to extract biophysical/biochemical information from hyperspectral remote sensor data. It is also important to know the type of land cover (e.g. vegetation type) found within the pixel. Classification of land cover using hyperspectral data is often performed using algorithms, such as the spectral angle mapper (Jensen 2005). In addition, subpixel classification (processing) can be performed using spectral mixture analysis algorithms that provide statistics on the proportion (abundance) of materials found within a pixel, for example, 33% corn,

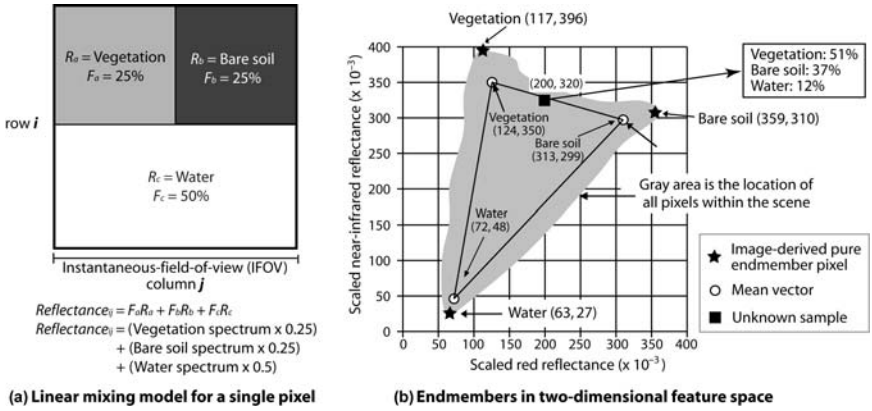

Fig. 6. Example of subpixel spectral mixture analysis used to extract the fraction of a specific material within a pixel (modified from Jensen 2005).

67% bare soil (Okin et al. 2001). This proportional land-cover information can be used in conjunction with the remote sensing-derived biophysical information to provide a more complete inventory of the characteristics of individual picture elements. This section briefly reviews subpixel spectral mixture analysis focusing on vegetation applications.

SUBPIXEL ANALYSIS TO ESTIMATE ABUNDANCE OF VEGETATION

Subpixel processing that extracts the amount (proportion) of a specific material within a pixel from a hyperspectral image cube has been widely used in forest, agriculture, and geology. A spectral *endmember*, the spectral reflectance curve for a pure material (e.g. bare soil) in the landscape, is used for subpixel processing. Subpixel spectral mixture analysis estimates the fractions of each spectral endmember within a pixel (Jensen 2005). For example, spectral reflectance from a pixel may be a spectral combination of three materials (e.g. vegetation, bare soil, and water) located within the pixel (Figure 6). A linear mixing model is generally applied to subpixel analysis using the following rules:

$$Reflectance_{ij} = \sum_{k=1}^{n} F_k \cdot R_k + E_{ij}, \text{ where}$$

$$\sum_{k=1}^{n} F_k = 1$$

$Reflectance_{ij}$ is the apparent surface reflectance of the pixel at location i, j under investigation, F_k is the fraction of endmember k, R_k is the reflectance of endmember k, n is the number of spectral endmembers found in the scene, and E_{ij} represents the residual error.

Figure 6B shows the location of endmember and hypothetical mean vectors associated with three materials (i.e. vegetation, bare soil, water) in red and near-infrared spectral reflectance feature space. For example, if we have a sample pixel with the reflectance of (200, 320), then the abundance of vegetation, bare soil, and water endmembers can be calculated using the above equations assuming that the data have no noise (i.e. vegetation: 51%, bare soil: 37%, water: 12%). This logic has been widely applied to subpixel classification and spatial pattern analysis of materials using multispectral and/or hyperspectral remote sensing data. It is particularly useful for hyperspectral remote sensing data, because the data generally have many more bands than the endmembers under investigation. However, many scientists point out that it is often difficult to extract all of the pure endmembers of materials under investigation (Jensen et al. 2009).

Subpixel spectral mixture analysis has been applied to vegetation mapping and spatial pattern analysis. McGwire et al. (2000) compared two approaches to estimation of vegetation percent cover: endmember-derived abundance indices versus narrow-band and broadband vegetation indices (e.g. NDVI, SAVI). They found that the fractions using endmembers (i.e. vegetation, soil, and shadow) were more highly correlated with vegetation percent cover. Subpixel analysis was adopted to analyze spatial patterns of forest fuels from AVIRIS hyperspectral data by Jia et al. (2006). Based on the abundance images of the three forest fuel components (i.e. photosynthetic vegetation, non-photosynthetic vegetation, and bare soil), the spatial patterns of vegetation and fuel characteristics at a local scale were assessed.

Conclusions

Hand-held spectroradiometers and hyperspectral remote sensing systems can provide valuable spectral information that can be used to measure the type, amount, and functional health of vegetation. This article first briefly reviewed several fundamental principles associated with *in situ* and remote sensing spectroradiometry. The article then focused on (i) the modeling techniques often applied to hyperspectral measurements to predict foliar and canopy characteristics, including statistical regression methods, spectral positioning methods, physical models, and artificial intelligence, and (ii) hyperspectral vegetation mapping and spatial pattern analysis, including subpixel classification. These modeling and classification approaches have produced successful results in many vegetation applications. However, it should be noted that there is no single method that can be successfully applied to all types of hyperspectral data and to all vegetation environments. Ultraspectral remote sensing involving many hundreds of bands is on the horizon. New methods and algorithms will be required to extract accurate vegetation information from improved hyper- and ultraspectral data.

Short Biographies

Jungho Im is an Assistant Professor of Environmental Resources and Forest Engineering at the State University of New York, College of Environmental Science and Forestry, Syracuse, New York, USA. He holds a master degree in environmental management from Seoul National University, South Korea, and a PhD in Geography, specializing in remote sensing and geographic information systems (GIS) from the University of South Carolina, USA. His research interests include (i) algorithm development using GIS and remote sensing technologies to model environmental processes, (ii) advanced remote sensing data assimilation, and (iii) monitoring systems for sustainable development of land resources. He has authored papers on diverse subjects in *Remote Sensing of Environment*, *International Journal of Remote Sensing*, *Photogrammetric Engineering & Remote Sensing*, *Geocarto International*, and *GIScience & Remote Sensing*.

John R. Jensen is a Carolina Distinguished Professor of Geography at the University of South Carolina, USA. He received his masters degree from Brigham Young University and his PhD from University of California, Los Angeles, specializing in analytical cartography and remote sensing of the environment. His research interests include the development of improved digital image processing algorithms for the extraction of biophysical and land-cover information from remote sensor data and documenting change through time. He is a member of the National Academy of Sciences Mapping Science Committee. He is a Past-President and a Certified Photogrammetrist with the American Society for Photogrammetry & Remote Sensing. He has authored numerous papers in *Remote Sensing of Environment*, *International Journal of Remote Sensing*, *Photogrammetric Engineering & Remote Sensing*, *Geocarto International*, and *GIScience & Remote Sensing*.

Note

* Correspondence address: Jungho Im, Department of Environmental Resources & Forest Engineering, State University of New York, College of Environmental Science & Forestry, Syracuse, NY 13210, USA. E-mail: imj@esf.edu.

References

Aparicio, N., et al. (2000). Spectral vegetation indices as non-destructive tools for determining durum wheat yield. *Agronomy Journal* 92, pp. 83–91.

Baranoski, G. V., and Rokne, J. G. (2005). A practical approach for estimating the red edge position of plant leaf reflectance. *International Journal of Remote Sensing* 26 (3), pp. 503–521.

Beeri, O., et al. (2007). Estimating forage quantity and quality using aerial hyperspectral imagery for northern mixed-grass prairie. *Remote Sensing of Environment* 110, pp. 216–225.

Blackburn, G. A., and Ferwerda, J. G. (2008). Retrieval of chlorophyll concentration from leaf reflectance spectra using wavelet analysis. *Remote Sensing of Environment* 112, pp. 1614–1632.

Boegh, E., et al. (2002). Airborne multispectral data for quantifying leaf area index, nitrogen concentration, and photosynthetic efficiency in agriculture. *Remote Sensing of Environment* 81, pp. 179–193.

Breiman, L., et al. (1984). *Classification and regression trees*. New York: Chapman and Hall.
Cheng, Y., et al. (2006). Estimating vegetation water content with hyperspectral data for different canopy scenarios: relationships between AVIRIS and MODIS indices. *Remote Sensing of Environment* 105, pp. 354–366.
Chirici, G., Barbati, A., and Maselli, F. (2007). Modeling of Italian forest net primary productivity by the integration of remotely sensed and GIS data. *Forest Ecology and Management* 246, pp. 285–295.
Chmura, D. J., Rahman, M. S., and Tjoelker, M. G. (2007). Crown structure and biomass allocation patterns modulate aboveground productivity in young loblolly pine and slash pine. *Forest Ecology and Management* 243, pp. 219–230.
Cho, M. A., and Skidmore, A. K. (2006). A new technique for extracting the red edge position from hyperspectral data: the linear extrapolation method. *Remote Sensing of Environment* 101, pp. 181–193.
Colombo, R., et al. (2003). Retrieval of leaf area index in different vegetation types using high resolution satellite data. *Remote Sensing of Environment* 86, pp. 120–131.
——. (2008). Estimation of leaf and canopy water content in poplar plantations by means of hyperspectral indices and inverse modeling. *Remote Sensing of Environment* 112, pp. 1820–1834.
Curran, P. J., Windham, W. R., and Gholz, H. L. (1995). Exploring the relationship between reflectance red edge and chlorophyll content in slash pine leaves. *Tree Physiology* 15, pp. 203–206.
Darvishzadeh, R., et al. (2008). Inversion of a radiative transfer model for estimating vegetation LAI and chlorophyll in heterogeneous grassland. *Remote Sensing of Environment* 112, pp. 2592–2604.
Dawson, T. P., and Curran, P. J. (1998). A new technique for interpolating the reflectance red edge position. *International Journal of Remote Sensing* 19 (11), pp. 2133–2139.
Dawson, T. P., Curran, P., and Plummer, S. (1998). LIBERTY – Modeling the effects of leaf biochemical concentration on reflectance spectra. *Remote Sensing of Environment* 65, pp. 50–60.
Ferwerda, J. G., and Skidmore, A. K. (2007). Can nutrient status of four woody plant species be predicted using field spectrometry? *ISPRS Journal of Photogrammetry & Remote Sensing*, in press.
Filella, I., and Penuelas, J. (1994). The red edge position and shape as indicators of plant chlorophyll content, biomass and hydric status. *International Journal of Remote Sensing* 15 (7), pp. 1459–1470.
Food and Agriculture Organization. (2005). *Leaf area index*. Terrestrial Ecosystem Monitoring Sites. [online]. Retrieved on 26 June 2008 from http://www.fao.org/gtos/tems/variable_list.jsp
Galvao, L. S., Formaggio, A. R., and Tisot, D. A. (2005). Discrimination of surface varieties in Southeastern Brazil with EO-1 Hyperion data. *Remote Sensing of Environment* 94, pp. 523–534.
Garcia-Quijano, M. J. (2006). *Claycap anomaly detection using hyperspectral remote sensing and lidargrammetric techniques*. Ph.D. Dissertation, Department of Geography, University of South Carolina, Columbia, SC, USA.
Gitelson, A. A., et al. (2002). Novel algorithms for remote estimation of vegetation fraction. *Remote Sensing of Environment* 80, pp. 76–87.
Goetz, S. J. (2002). Recent advances in remote sensing of biophysical variables: an overview of the special issue. *Remote Sensing of Environment* 79, pp. 145–146.
Gong, P., Pu, R., and Heald, R. C. (2002). Analysis of *in situ* hyperspectral data for nutrient estimation of giant sequoia. *International Journal of Remote Sensing* 23, pp. 1827–1850.
Haboudane, D., et al. (2002). Integrated narrow-band vegetation indices for prediction of crop chlorophyll content for application to precision agriculture. *Remote Sensing of Environment* 81, pp. 416–426.
Hansen, P. M., and Schjoerring, J. K. (2003). Reflectance measurement of canopy biomass and nitrogen status in wheat crops using normalized difference vegetation indices and partial least squares regression. *Remote Sensing of Environment* 86, pp. 542–553.
Hengl, T. (2002). Neural network fundamentals: a neural computing primer. *Personal Computing Artificial Intelligence* 16 (3), pp. 32–43.

Horler, D. N., Dockray, N., and Barber, J. (1983). The red edge of plant leaf reflectance. *International Journal of Remote Sensing* 4 (2), pp. 273–288.

Hu, B., et al. (2004). Retrieval of crop chlorophyll content and leaf area index from decompressed hyperspectral data: the effects of data compression. *Remote Sensing of Environment* 92, pp. 139–152.

Huang, C., and Townshend, J. R. G. (2003). A stepwise regression tree for nonlinear approximation: applications to estimating subpixel land cover. *International Journal of Remote Sensing* 24, pp. 75–90.

Huete, A. R., and Liu, H. Q. (1994). An error and sensitivity analysis of the atmospheric and soil-correcting variants of the NDVI for the MODIS-EOS. *IEEE Transactions on Geoscience and Remote Sensing* 32 (4), pp. 897–905.

Huete, A. R., et al. (2002). Overview of the radiometric and biophysical performance of the MODIS vegetation indices. *Remote Sensing of Environment* 83, pp. 195–213.

Im, J., et al. (2008). Hyperspectral remote sensing analysis of short rotation woody crops grown with controlled nutrient and irrigation treatments. *Geocarto International* in press.

Jacquemoud, S., and Baret, F. (1990). PROSPECT: a model of leaf optical properties spectral. *Remote Sensing of Environment* 34, pp. 75–91.

Jensen, J. R. (2005). *Introductory digital image processing*. Upper Saddle River, NJ: Prentice-Hall, p. 526.

——. (2007). *Remote sensing of the environment*. Upper Saddle River, NJ: Prentice-Hall, p. 592.

Jensen, J. R., et al. (1998). Extraction of smooth Cordgrass (*Spartina Alterniflora*) biomass and LAI parameters from high resolution imagery. *Geocarto International* 13 (4), pp. 25–34.

——. (2002). Remote sensing of biomass, leaf-area-index, and chlorophyll a and b content in the ACE basin national estuarine research reserve using sub-meter digital camera imagery. *Geocarto international* 17 (3), pp. 25–34.

——. (2009). Chapter 18. Image classification. In: Warner, T., Nellis, D. and Foody, G. (eds) *The SAGE handbook of remote sensing*. Thousand Oaks, CA: Sage.

Jensen, J. R., Qiu, F., and Ji, M. (1999). Predictive modeling of coniferous forest age using statistical and artificial neural network approaches applied to remote sensing data. *International Journal of Remote Sensing* 20 (14), pp. 2805–2822.

Jia, G. J., et al. (2006). Assessing spatial patterns of forest fuel using AVIRIS data. *Remote Sensing of Environment* 102, pp. 318–327.

Johnson, L. F., Hlavaka, C. A., and Peterson, D. L. (1994). Multivariate analysis of AVIRIS data for canopy biochemical estimation along the Oregon transect. *Remote Sensing of Environment* 47, pp. 216–230.

Jokela, A., et al. (1997). Effects of foliar potassium concentration on morphology, ultrastructure and polyamine concentrations of Scots pine needles. *Tree Physiology* 17, pp. 677–685.

Kokaly, R. F., et al. (2003). Mapping vegetation in Yellowstone National Park using spectral feature analysis of AVIRIS data. *Remote Sensing of Environment* 84, pp. 437–456.

McGwire, K., Minor, T., and Fenstermaker, L. (2000). Hyperspectral mixture modeling for quantifying sparse vegetation cover in arid environments. *Remote Sensing of Environment* 72, pp. 360–374.

Miller, J. R., Hare, E. W., and Wu, J. (1990). Quantitative characterization of the red edge reflectance 1. An inverted-Gaussian model. *International Journal of Remote Sensing* 11 (10), pp. 1755–1773.

Milton, N. M., Eiswerth, B. A., and Ager, C. M. (1991). Effect of phosphorus deficiency on spectral reflectance and morphology of soybean plants. *Remote Sensing of Environment* 36, pp. 121–127.

Moisen, G. G., et al. (2006). Predicting tree species presence and basal area in Utah: a comparison of stochastic gradient boosting, generalized additive models, and tree-based methods. *Ecological Modeling* 199, pp. 176–187.

Moorthy, I., Miller, J. R., and Noland, T. L., (2008). Estimating chlorophyll concentration in conifer needles with hyperspectral data: an assessment at the needle and canopy level. *Remote Sensing of Environment* 112, pp. 2824–2838.

Mutanga, O., Skidmore, A. K., and Prins, H. H. (2003). Predicting *in situ* pasture quality in the Kruger National Park, South Africa, using continuum-removed absorption features. *Remote Sensing of Environment* 89, pp. 393–408.

Nolin, A. W., and Dozier, J., (2000). A hyperspectral method for remotely sensing the grain size of snow. *Remote Sensing of Environment* 74, pp. 207–216.

Okin, G. S., et al. (2001). Practical limits on hyperspectral vegetation discrimination in arid and semiarid environments. *Remote Sensing of Environment* 77, pp. 212–225.

Perry, E. M., and Davenport, J. R. (2007). Spectral and spatial differences in response of vegetation indices to nitrogen treatments on apple. *Computers and Electronics in Agriculture* 59, pp. 56–65.

Pinar, A., and Curran, P. J. (1996). Grass chlorophyll and the reflectance red edge. *International Journal of Remote Sensing* 17 (2), pp. 351–357.

Sims, D., and Gamon, J. (2002). Relationships between leaf pigment content and spectral reflectance across a wide range of species, leaf structures and developmental stages. *Remote Sensing of Environment* 81, pp. 337–354.

Smith, K. L., Steven, M. D., and Colls, J. J. (2004). Use of hyperspectral derivative ratios in the red-edge region to identify plant stress responses to gas leaks. *Remote Sensing of Environment* 92, pp. 207–217.

Tilling, A. K., et al. (2007). Remote sensing of nitrogen and water stress in wheat. *Field Crops Research* 104, pp. 77–85.

Townsend, P. A., et al. (2003). Application of imaging spectroscopy to mapping canopy nitrogen in the forests of the central Appalachian mountains using Hyperion and AVIRIS. *IEEE Transactions on Geoscience and Remote Sensing* 41 (6), pp. 1347–1354.

Trombetti, M., et al. (2008). Multi-temporal vegetation canopy water content retrieval and interpretation using artificial neural networks for the continental USA. *Remote Sensing of Environment* 112, pp. 203–215.

Verger, A., Baret, F., and Weiss, M., (2008). Performance of neural networks for deriving LAI estimates from existing CYCLOPES and MODIS products. *Remote Sensing of Environment* 112, pp. 2789–2803.

Verhoef, W. (1984). Light scattering by leaf layers with application to canopy reflectance modeling: the SAIL model. *Remote Sensing of Environment* 16, pp. 125–141.

Walthall, C., et al. (2004). A comparison of empirical and neural network approaches for estimating corn and soybean leaf area index from Landsat ETM+ imagery. *Remote Sensing of Environment* 92, pp. 465–474.

Wu, C., et al. (2008). Estimating chlorophyll content from hyperspectral vegetation indices: modeling and validation. *Agricultural and Forest Meteorology* 148, pp. 1230–1241.

Ye, X., et al. (2006). Estimation of citrus yield from airborne hyperspectral images using a neural network model. *Ecological Modeling* 198, pp. 426–432.